

Effects of inert gas (Ne) on thermal convection of mercurous chloride system of Hg_2Cl_2 and Ne during physical vapor transport

Jeong-Gil Choi[†], Kyong-Hwan Lee* and Geug-Tae Kim

Department of Nano-Bio Chemical Engineering, Hannam University, Daejeon 305-811, Korea

**Clean Energy Research Department, Korea Institute of Energy Research, Daejeon 305-343, Korea*

(Received September 29, 2008)

(Accepted October 27, 2008)

Abstract For an aspect ratio (transport length-to-width) of 5, $\text{Pr} = 1.13$, $\text{Le} = 1.91$, $\text{Pe} = 4.3$, $\text{Cv} = 1.01$, $P_B = 20$ Torr, the effects of addition of inert gas Ne on thermally buoyancy-driven convection ($\text{Gr} = 2.44 \times 10^3$) are numerically investigated for further understanding and insight into essence of transport phenomena in two dimensional horizontal enclosures. For $10 \text{ K} \leq \Delta T \leq 50 \text{ K}$, the crystal growth rate increases from 10 K up to 20 K, and then is slowly decreased until $\Delta T = 50 \text{ K}$, which is likely to be due to the effects of thermo-physical properties stronger than the temperature gradient corresponding to driving force for thermal convection. The dimensional maximum velocity gratitude reflecting the intensity of thermal convection is directly and linearly proportional to the temperature difference between the source and crystal regions. The rate is first order-exponentially decreased for $2 \leq \text{Ar} \leq 5$. This is related to the finding that the effects of side walls tend to stabilize convection in the growth reactor. In addition, the rate is first order exponentially decayed for $10 \leq P_B \leq 200$ Torr.

Key words Mercurous chloride, Thermally buoyancy-driven convection, Neon and physical vapor transport

1. Introduction

Mercurous chloride (Hg_2Cl_2) materials are important for applications in acousto-optic and opto-electronic devices such as Bragg cells, X-ray detectors operating at ambient temperature [1]. The equimolar Hg_2Cl_2 compound decomposes to two liquids at a temperature near 525°C where the vapor pressure is above 20 atm [2, 3]. Because of this decomposition and high vapor pressure, Hg_2Cl_2 cannot be solidified as a single crystal directly from the stoichiometric melt. However, very similar to the mercurous bromide, mercurous chloride exhibits sufficiently high vapor pressure at low temperatures so that these crystals are usually grown by the physical vapor transport (PVT) in closed silica glass ampoules. The PVT processing has many advantages over melt-growth methods since it can be conducted at low temperatures: (1) vapor-solid interfaces possess relatively high interfacial morphological stability against non-uniformities in heat and mass transfer; (2) high purity crystals are achieved; (3) materials decomposed before melting, such as Hg_2Cl_2 can be grown; (4) lower point defect and dislocation densities are achieved [4]. The mechanism of the PVT process is simple: sublimation-condensation

in closed silica glass ampoules in temperature gradient imposed between the source material and the growing crystal. In the actual PVT system of Hg_2Cl_2 , the molecular species Hg_2Cl_2 sublimates as the vapor phase from the crystalline source material (Hg_2Cl_2), and is subsequently transported and re-incorporated into the single crystalline phase (Hg_2Cl_2) [5]. Recently, PVT has become an important crystal growth process for a variety of acousto-optic materials. However, the industrial applications of the PVT process remain limited. One of important main reasons is that transport phenomena occurring in the vapor are complex and coupled so that it is difficult to design or control the process accurately. Such complexity and coupling are associated with the inevitable occurrence of thermal and/or solutal convection generated by the interaction of gravity with density gradients arising from temperature and/or concentration gradients. In general, convection has been regarded as detrimental and, thus, to be avoided or minimized in PVT growth system. These thermal and/or solutal convection-induced complications result in problems ranging from crystal inhomogeneity to structural imperfection. Therefore, in order to analyze and control the PVT process accurately, and also make significant improvements in the process, it is essential to investigate the roles of convection in the PVT process.

Markham, Greenwell and Rosenberger [6] examined the effects of thermal and thermo-solutal convections

[†]Corresponding author

Tel: +82-42-629-8841

Fax: +82-42-629-8835

E-mail: choi1002@hotmail.com

during the PVT process inside vertical cylindrical enclosures for a time-independent system, and showed that even in the absence of gravity, convection can be present, causing nonuniform concentration gradients. They emphasized the role of geometry in the analysis of the effects of convection. As such these fundamentally constitute steady state two-dimensional models. The steady state models are limited to low Rayleigh number applications, because the oscillation of the flow field occurs as the Rayleigh number increases. To address the issue of unsteady flows in PVT, Duval [7] performed a numerical study on transient thermal convection in the PVT processing of Hg_2Cl_2 very similar to the mercurous bromide for a vertical rectangular enclosure with insulated temperature boundary conditions for Rayleigh numbers up to 10^6 . Nadarajah *et al.* [8] addressed the effects of solutal convection for any significant disparity in the molecular weights of the crystal components and the inert gas. Zhou *et al.* [9] reported that the traditional approach of calculating the mass flux assuming one-dimensional flow for low vapor pressure systems is indeed correct. Rosenberger *et al.* [10] studied three-dimensional numerical modeling of the PVT yielded quantitative agreement with measured transport rates of iodine through octofluorocyclobutane (C_4F_8) as inert background gas in horizontal cylindrical ampoules.

In this theoretical study, a two-dimensional model is used for the analysis of the PVT processes during vapor-growth of mercurous chloride crystals (Hg_2Cl_2) in horizontally oriented, cylindrical, closed ampoules in a two-zone furnace system. Diffusion-limited processes are considered in this paper, although the recent paper of Singh, Mazelsky and Glicksman [11] demonstrated that the interface kinetics plays an important role in the PVT system of Hg_2Cl_2 . Thermally buoyancy-driven convection will be considered at this point, primarily for a mixture of Hg_2Cl_2 vapor and impurity of Neon (Ne), although solutally-induced convection is more important than thermal convection in some cases.

It is the purpose of this paper to relate applied thermally buoyancy-driven convection process parameters such as the temperature differences between the source and crystal region, aspect ratio (transport length -to-width), and the partial pressure of component B, P_B (Torr) to the crystal growth rate and the maximum velocity magnitude to examine the effects of the addition of inert gas (Ne) on thermally buoyancy-driven convection in order to gain insights into the underlying physicochemical processes.

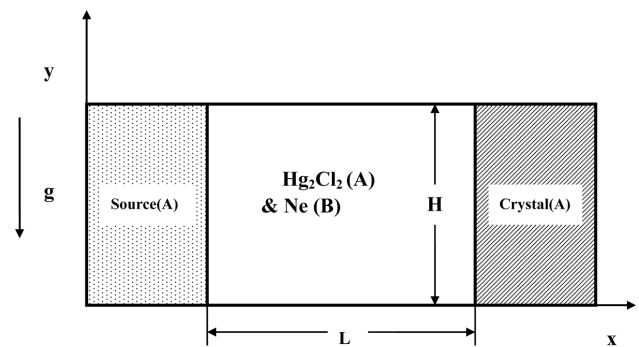


Fig. 1. Schematic of PVT growth reactor in a two-dimensional rectangular system.

2. Physical and Mathematical Formulations

Consider a rectangular enclosure of height H and transport length L , shown in Fig. 1. The source is maintained at a temperature T_s , while the growing crystal is at a temperature T_c , with $T_s > T_c$. PVT of the transported component A (Hg_2Cl_2) occurs inevitably, due to presence of impurities, with the presence of a component B (Ne). The interfaces are assumed to be flat for simplicity. The finite normal velocities at the interfaces can be expressed by Stefan flow deduced from the one-dimensional diffusion-limited model [12], which would provide the coupling between the fluid dynamics and species calculations. On the other hand, the tangential component of the mass average velocity of the vapor at the interfaces vanishes. Thermodynamic equilibria are assumed at the interfaces so that the mass fractions at the interfaces are kept constant at $\omega_{A,s}$ and $\omega_{A,c}$. On the vertical non-reacting walls appropriate velocity boundary conditions are no-slip, the normal concentration gradients are zero, and wall temperatures are imposed as nonlinear temperature gradients.

Thermo-physical properties of the fluid are assumed to be constant, except for the density. When the Boussinesq approximation is invoked, density is assumed constant except the buoyancy body force term. The density is assumed to be a function of both temperature and concentration. The ideal gas law and Dalton's law of partial pressures are used. Viscous energy dissipation and the Soret-Dufour (thermo-diffusion) effects can be neglected, as their contributions remain relatively insignificant for the conditions encountered in our PVT crystal growth processes. Radiative heat transfer can be neglected under our conditions, based on Kassemi and Duval [13].

The transport of fluid within a rectangular PVT crys-

tal growth reactor is governed by a system of elliptic, coupled conservation equations for mass (continuity), momentum, energy and species (diffusion) with their appropriate boundary conditions. Let u_x , u_y denote the velocity components along the x - and y -coordinates in the x , y rectangular coordinate, and let T , ω_A , p denote the temperature, mass fraction of species A (Hg₂Cl₂) and pressure, respectively.

The dimensionless variables are defined as follows:

$$x^* = \frac{x}{H}, \quad y^* = \frac{y}{H}, \quad (1)$$

$$u^* = \frac{u_x}{U_c}, \quad v^* = \frac{u_y}{U_c}, \quad p^* = \frac{p}{\rho_c U_c^2}, \quad (2)$$

$$T^* = \frac{T - T_c}{T_s - T_c}, \quad \omega_A^* = \frac{\omega_A - \omega_{A,c}}{\omega_{A,s} - \omega_{A,c}}. \quad (3)$$

The dimensionless governing equations are given by:

$$\nabla^* \cdot \mathbf{V}^* = 0, \quad (4)$$

$$\vec{\nabla}^* \cdot \nabla^* \vec{V}^* = -V^* p^* + \text{Pr} \nabla^{*2} \vec{V}^* - \text{Ra} \cdot \text{Pr} \cdot T^* \cdot \mathbf{e}_g, \quad (5)$$

$$\vec{\nabla}^* \cdot \nabla^* T^* = \nabla^{*2} T^* \quad (6)$$

$$\vec{\nabla}^* \cdot \nabla^* \omega_A^* = \frac{1}{\text{Le}} \nabla^{*2} \omega_A^* \quad (7)$$

These nonlinear, coupled sets of equations are numerically integrated with the following boundary conditions:

On the walls ($0 < x^* < L/H$, $y^* = 0$ and 1):

$$u^*(x^*, 0) = u^*(x^*, 1) = v^*(x^*, 0) = v^*(x^*, 1) = 0 \quad (8)$$

$$\frac{\partial \omega_A^*(x^*, 0)}{\partial y^*} = \frac{\partial \omega_A^*(x^*, 1)}{\partial y^*} = 0,$$

$$T^*(x^*, 0) = T^*(x^*, 1) = \frac{T - T_c}{T_s - T_c}$$

On the source ($x^* = 0$, $0 < y^* < 1$):

$$u^*(0, y^*) = -\frac{1}{\text{Le}(1 - \omega_{A,s})} \frac{\Delta \omega}{\partial x^*} \frac{\partial \omega_A^*(0, y^*)}{\partial x^*}, \quad (9)$$

$$v^*(0, y^*) = 0,$$

$$T^*(0, y^*) = 1,$$

$$\omega_A^*(0, y^*) = 1.$$

On the crystal ($x^* = L/H$, $0 < y^* < 1$):

$$u^*(L/H, y^*) = -\frac{1}{\text{Le}(1 - \omega_{A,c})} \frac{\Delta \omega}{\partial x^*} \frac{\partial \omega_A^*(L/H, y^*)}{\partial x^*}, \quad (10)$$

$$v^*(L/H, y^*) = 0,$$

$$T^*(L/H, y^*) = 0,$$

$$\omega_A^*(L/H, y^*) = 0.$$

In the dimensionless parameters in the governing equations the thermo-physical properties of the gas mixture are estimated from gas kinetic theory using Chapman-Enskog's formulas [14].

The vapor pressure [15] p_A of Hg₂Cl₂ (in the unit of Pascal) can be evaluated from the

$$p_A = e^{(a-b/T)}, \quad (11)$$

following formula as a function of temperature: in which $a = 29.75$, $b = 11767.1$.

The crystal growth rate V_c is calculated from a mass balance at the crystal vapor interface, assuming fast kinetics, i.e. all the vapor is incorporated into the crystal, which is given by (subscripts c , v refer to crystal and vapor, respectively)

$$\int \rho_v v_v \cdot n dA = \int \rho_c v_c \cdot n dA, \quad (12)$$

$$v_c = \frac{\rho_v \int v_v \cdot n dA}{\rho_c \int dA}. \quad (13)$$

The detailed numerical schemes in order to solve the discretization equations for the system of nonlinear, coupled governing partial differential equations are found in [16].

3. Results and Discussion

The purposes for this study is to correlate the growth rate to process parameters such as an aspect ratio, a partial pressure of component B to investigate the effects of inert gas Ne on thermal convection during physical vapor transport. Thus, it is desirable to express some results in terms of dimensional growth rate, however they are also applicable to parameter ranges over which the process varies in the manner given. The six dimensionless parameters, namely Gr , Ar , Pr , Le , C_v and Pe , are independent and arise naturally from the dimensionless governing equations and boundary conditions. The dimensionless parameters and physical properties for the operating conditions of this study are shown in Table 1.

When the molecular weight of a light element (Ne) is not equal to that of the crystal component (Hg₂Cl₂) during the physical vapor transport, both solutal and/or ther-

Table 1
Typical thermo-physical properties used in this study ($M_A = 472.086$, $M_B = 20.183$)

Transport length, L	10 cm
Height, H	2 cm
Source temperature, T_s	350°C
Crystal temperature, T_c	300°C
Density, ρ	0.00178 g/cm ³
Dynamic viscosity, μ	0.00028 g/(cm·sec)
Diffusivity, D_{AB}	0.82 cm ² /s
Thermal expansion coefficient, β	0.0016 K ⁻¹
Prandtl number, Pr	1.13
Lewis number, Le	0.019
Peclet, Pe	4.3
Concentration number, Cv	1.01
Total system pressure, P_T	413.06 Torr
Partial pressure of component B, P_B	20 Torr
Thermal Grashof number, Gr	2.44×10^3

mal effects should be considered. But, solutal convection would be assumed to be negligible by setting the molecular weight of component B (Ne) equal to that of the component A, Hg_2Cl_2 at density term in Eq. (5). Conductive wall boundary conditions are considered, while the insulated walls are not considered because it is difficult to obtain in practice and most of vapor growth experiments. In addition, a nonlinear thermal profile (“hump”) imposed at the walls is not considered at this point which can be obtained by an often used experimental technique to prevent undesirable nucleations [17,

18]. In general, this temperature hump could eliminate the problem of vapor supersaturation along the transport path and, thus, of parasitic nucleations at the walls. But, these humps may result in sharp temperature gradients near the crystal region, inducing thermal stresses and a decrease in crystal quality.

Fig. 2 shows the growth rates of Hg_2Cl_2 as a function of the temperature difference between the source and the crystal region, ΔT (K), for $10 \text{ K} \leq \Delta T \leq 50 \text{ K}$, with a linear conducting wall temperature profile. In general, with a linear temperature profile, the vapor of component A (Hg_2Cl_2) is in a supersaturation throughout the ampoule [19]. For $10 \text{ K} \leq \Delta T \leq 20 \text{ K}$, the growth rate slowly increases and, then is decreased gradually until $\Delta T = 50 \text{ K}$. The occurrence of this critical point near $\Delta T = 20 \text{ K}$ is likely to be due to the effects of thermo-physical properties stronger than the temperature gradient corresponding to driving force for thermal convection, as discussed later. Fig. 3 shows the direct and linear relationship between the Grashof number, Gr and the temperature difference, ΔT , corresponding to Fig. 2. Fig. 4 shows the dimensional maximum velocity magnitude, $|U|_{\max}$ is proportional to the temperature difference ΔT , which corresponds to Fig. 2. Note the dimensional maximum velocity magnitude, $|U|_{\max}$ implies the importance of intensity of convection during physical vapor transport. Fig. 5 the growth rates of Hg_2Cl_2 as a function of the dimensional Grashof number, Gr , for $10 \text{ K} \leq$

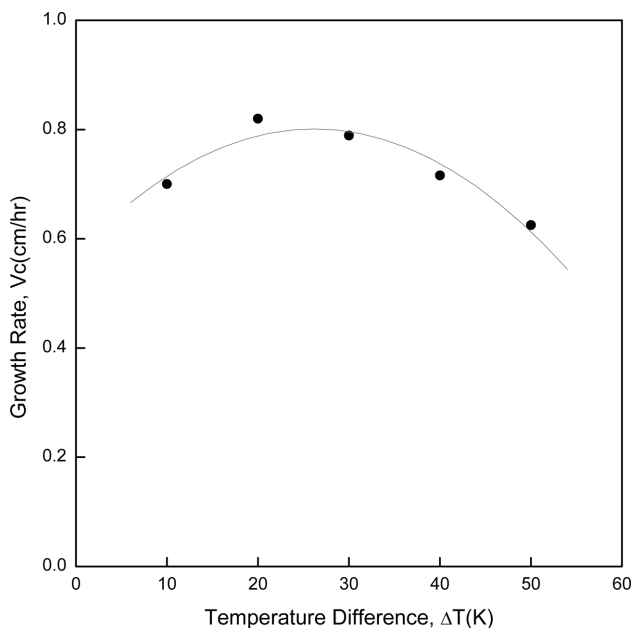


Fig. 2. Growth rates of Hg_2Cl_2 as a function of the temperature difference between the source and the crystal region, ΔT (K), for $10 \text{ K} \leq \Delta T \leq 50 \text{ K}$, $Ar = 5$, $P_B = 20 \text{ Torr}$.

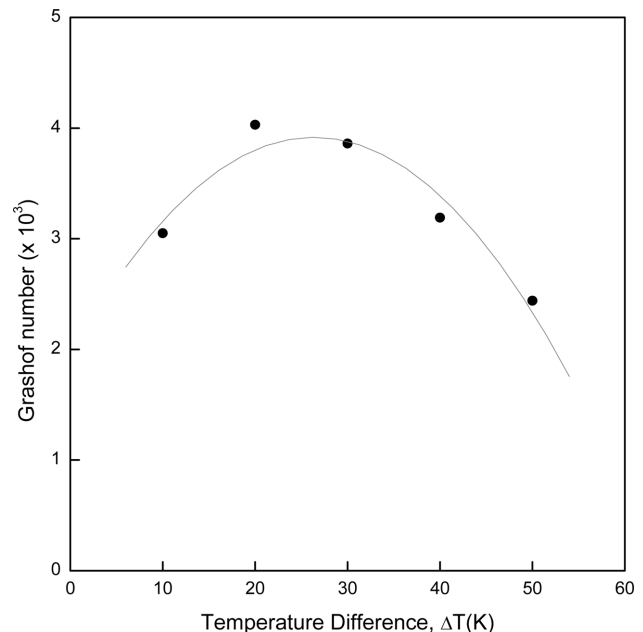


Fig. 3. Relationship between the dimensionless Grashof number, Gr and the temperature difference between the source and the crystal region, ΔT (K), corresponding to Fig. 2.

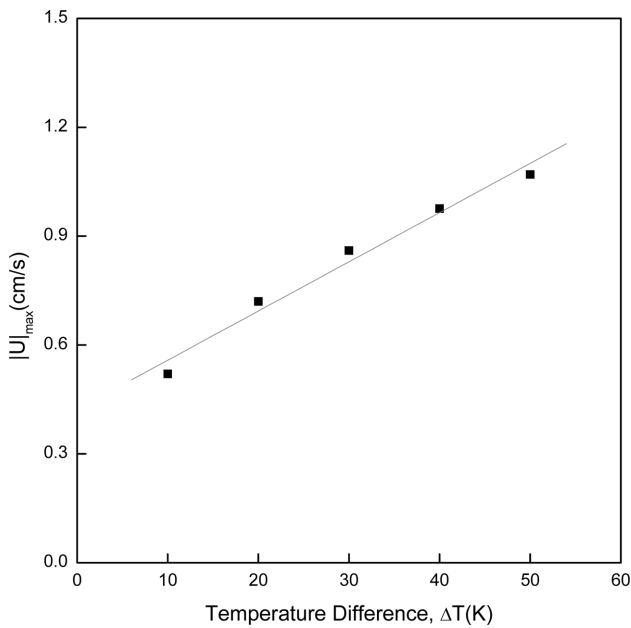


Fig. 4. The $|U|_{\max}$ as a function of the temperature difference between the source and the crystal region, ΔT (K), corresponding to Fig. 2.

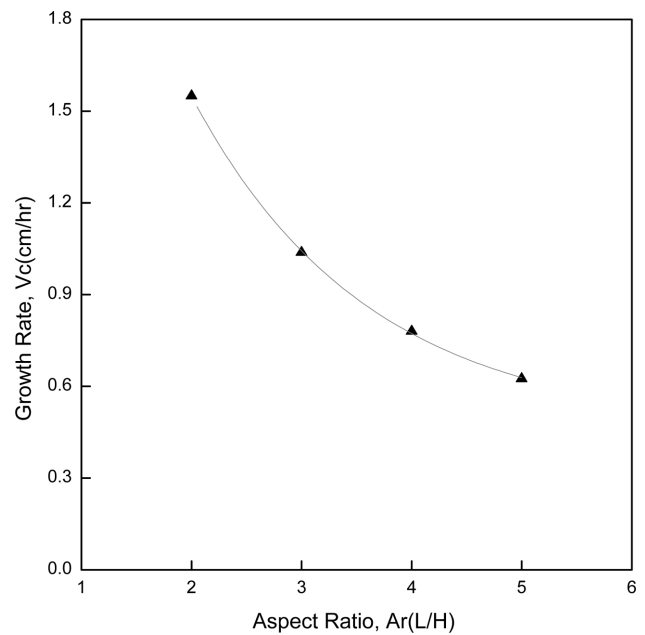


Fig. 6. Effects of aspect ratio Ar (L/H) on the crystal growth rates of Hg_2Cl_2 , with the height, H fixed.

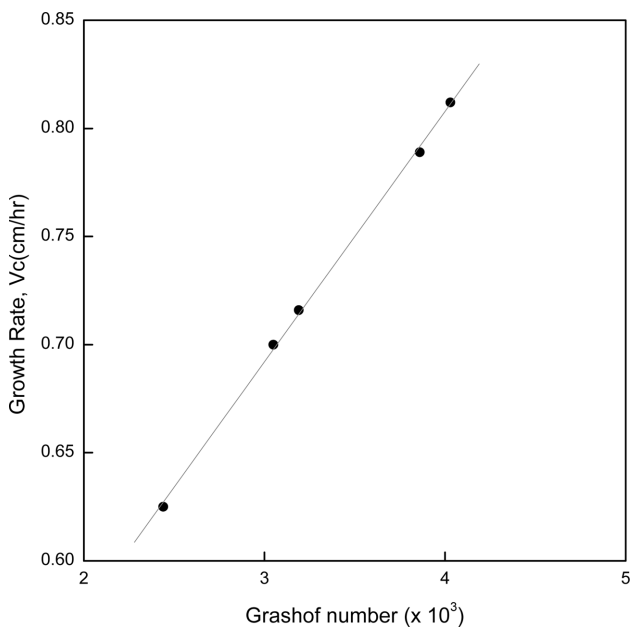


Fig. 5. Growth rates of Hg_2Cl_2 as a function of the dimensionless Grashof number, corresponding to Fig. 2.

$\Delta T \leq 50$ K. From the viewpoint of crystal growth rate, the rate is directly and intimately dependent on the Grashof number and $|U|_{\max}$ rather than the driving force of crystal growth, the temperature difference ΔT . Therefore, the Grashof number reflects both the effects of thermo-physical properties and the temperature gradient. Comparison of Fig. 2 with 5 supports the occurrence of this critical point near at $\Delta T = 20$ K is likely to

be due to the effects of thermo-physical properties stronger than the temperature gradient. Figs. 2 through 5 are based on $Ar = 5$, $P_B = 20$ Torr. For the case of $\Delta T = 50$ K, $Ar = 5$, $P_B = 20$ Torr, the corresponding five dimensionless parameters are $Pr = 1.133$, $Le = 1.91$, $Pe = 4.3$, $Cv = 1.01$, Gr (Grashof number) $= 2.44 \times 10^3$.

Fig. 6 shows the growth rates of Hg_2Cl_2 as a function of the aspect ratio, Ar (L/H) for $\Delta T = 50$ K, $P_B = 20$ Torr, with fixed width H. The rate is first order-exponentially decayed with the aspect ratio, Ar (L/H). This is intimately related with the effects of side walls which suppress the convection flow inside the growth enclosure. It is not surprising that the effects of side walls tend to stabilize convection in the growth reactor. This tendency is consistent with the results [20] on the pure thermal convection without crystal growth in enclosures. The rate is decreased sharply for the range from $Ar = 2$ to 3 by a factor of 0.66, and then for $3 \leq Ar \leq 5$, is decreased by a factor of 0.6. Note the numerical executions for $1 \leq Ar \leq 1.7$ cannot be performed, which is likely to be chaotic flows. As shown in Fig. 7, $|U|_{\max}$ has the same trend and decreasing degree as the rate against the aspect ratio. In other words, the decreasing degree is approximately 0.66 for $2 \leq Ar \leq 3$, and 0.60 for $3 \leq Ar \leq 5$, respectively. Note in actual crystal growth systems, the temperature profile is intimately related to the aspect ratio because the temperature profile is so imposed that it could not be altered. In this study, the conducting wall boundary conditions are used for the thermal boundary

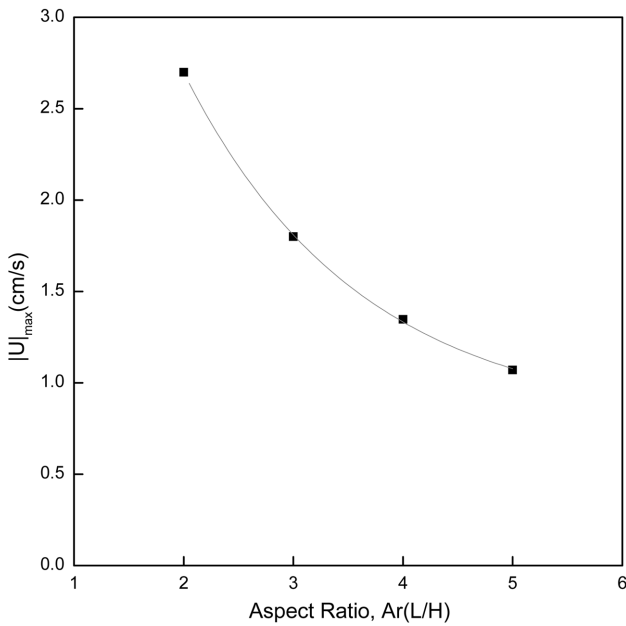


Fig. 7. The $|U|_{\max}$ as a function of the aspect ratio Ar (L/H), corresponding to Fig. 6.

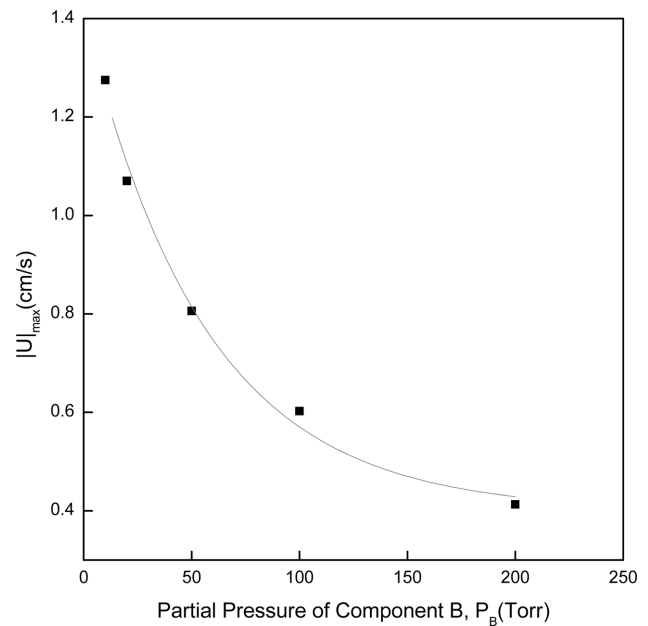


Fig. 9. The $|U|_{\max}$ as a function of the aspect ratio Ar (L/H), corresponding to Fig. 8.

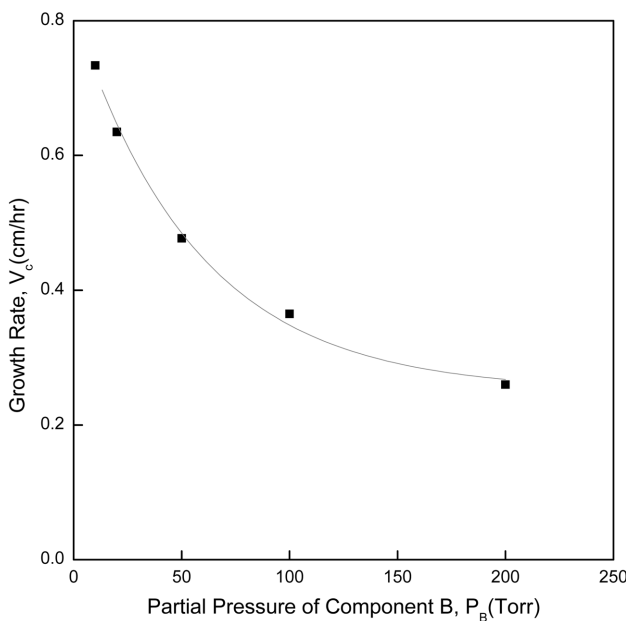


Fig. 8. Effects of partial pressure of component B, P_B (Torr) on the crystal growth rates of Hg_2Cl_2 .

conditions at walls and the temperature profiles are linear. Figs. 6 and 7 are based on $\Delta T = 50$ K and $P_B = 20$ Torr.

Fig. 8 shows the growth rates of Hg_2Cl_2 as a function of partial pressure of component B, P_B (Torr) for $\Delta T = 50$ K, $Ar = 5$. Like the case of aspect ratio, Ar (L/H), the rate is first order-exponentially decayed with P_B (Torr) for the range of $10 \text{ Torr} \leq P_B \leq 200 \text{ Torr}$. For

$10 \text{ Torr} \leq P_B \leq 50 \text{ Torr}$, the rate is decreased significantly by the factor of 0.65, and for $50 \text{ Torr} \leq P_B \leq 200 \text{ Torr}$, reduced by a factor of 0.55. As shown in Fig. 8, $|U|_{\max}$ has the same trend and decreasing degree as the rate against the partial pressure of component B, P_B (Torr). In other words, the decreasing degree is approximately 0.65 for $10 \text{ Torr} \leq P_B \leq 50 \text{ Torr}$, and 0.55 for $50 \text{ Torr} \leq P_B \leq 200 \text{ Torr}$, respectively. Comparisons of Figs. 2, 6 and 8 illustrate the side walls influence the most significant on the rate than thermal convective effects such the temperature difference, the partial pressure of component B. Figs. 8 and 9 are based on $\Delta T = 50$ K and $Ar = 5$.

4. Conclusions

The parameters under consideration in this study are $\Delta T = 50$ K, $Ar = 5$, $P_B = 20$ Torr, and the corresponding five dimensionless parameters of $Pr = 1.133$, $Le = 1.91$, $Pe = 4.3$, $Cv = 1.01$, Gr (Grashof number) $= 2.44 \times 10^3$. It is concluded that for $10 \text{ K} \leq \Delta T \leq 50 \text{ K}$, the crystal growth rate increases from 10 K up to 20 K, and then is slowly decreased until $\Delta T = 50$ K, which is likely to be due to the effects of thermo-physical properties stronger than the temperature gradient corresponding to driving force for thermal convection. The dimensional maximum velocity magnitude reflecting the intensity of thermal convection is directly and linearly proportional to

the temperature difference between the source and crystal regions. The rate is first order-exponentially decreased for $2 \leq \text{Ar} \leq 5$. This is related to the finding that the effects of side walls tend to stabilize convection in the growth reactor. In addition, the rate is first order exponentially decayed for $10 \leq P_B \leq 200$ Torr. Finally, the side walls are found to influence the most significant on the rate than thermal convective effects such the temperature difference, the partial pressure of component B.

Acknowledgement

The authors wish to appreciate the financial support provided by the Hannam University through the Kyobi program of research project number of 2008A058 (April 1, 2008 through March 31, 2009).

References

- [1] N.B. Singh, M. Gottlieb, G.B. Brandt, A.M. Stewart, R. Mazelsky and M.E. Glicksman, "Growth and characterization of mercurous halide crystals:mercurous bromide system", *J. Crystal Growth* 137 (1994) 155.
- [2] N.B. Singh, R.H. Hopkins, R. Mazelsky and J.J. Conroy, "Purification and growth of mercurous chloride single crystals", *J. Crystal Growth* 75 (1970) 173.
- [3] S.J. Yosim and S.W. Mayer, "The mercury-mercuric chloride system", *J. Phys. Chem.* 60 (1960) 909.
- [4] F. Rosenberger, "Fluid dynamics in crystal growth from vapors," *Physico-Chemical Hydro-dynamics* 1 (1980).
- [5] N.B. Singh, M. Gottlieb, A.P. Goutzoulis, R.H. Hopkins and R. Mazelsky, "Mercurous Bromide acousto-optic devices", *J. Crystal Growth* 89 (1988) 527.
- [6] B.L. Markham, D.W. Greenwell and F. Rosenberger, "Numerical modeling of diffusive-convective physical vapor transport in cylindrical vertical ampoules", *J. Crystal Growth* 51 (1981) 426.
- [7] W.M. B. Duval, "Convection in the physical vapor transport process-- I: Thermal", *J. Chemical Vapor Deposition* 2 (1994) 188.
- [8] A. Nadarajah, F. Rosenberger and J. Alexander, "Effects of buoyancy-driven flow and thermal boundary conditions on physical vapor transport", *J. Crystal Growth* 118 (1992) 49.
- [9] H. Zhou, A. Zebib, S. Trivedi and W.M.B. Duval, "Physical vapor transport of zinc-telluride by dissociative sublimation", *J. Crystal Growth* 167 (1996) 534.
- [10] F. Rosenberger, J. Ouazzani, I. Viohl and N. Buchan, "Physical vapor transport revised", *J. Crystal Growth* 171 (1997) 270.
- [11] N.B. Singh, R. Mazelsky and M.E. Glicksman, "Evaluation of transport conditions during PVT: mercurous chloride system", *PhysicoChemical Hydrodynamics* 11 (1989) 41.
- [12] F. Rosenberger and G. Müller, "Interfacial transport in crystal growth, a parameter comparison of convective effects", *J. Crystal Growth* 65 (1983) 91.
- [13] M. Kassemi and W.M.B. Duval, "Interaction of surface radiation with convection in crystal growth by physical vapor transport", *J. Thermophys. Heat Transfer* 4 (1989) 454.
- [14] R.B. Bird, W.E. Stewart and E.N. Lightfoot, *Transport Phenomena* (John Wiley and Sons, New York, NY, 1960).
- [15] C. Mennetrier and W.M.B. Duval, Thermal-solutal convection with conduction effects inside a rectangular enclosure, NASA Technical Memorandum 105371 (1991).
- [16] S.V. Patankar, *Numerical Heat Transfer and Fluid Flow* (Hemisphere Publishing Corp., Washington D.C., 1980).
- [17] N.B. Singh and W.M.B. Duval, Growth kinetics of physical vapor transport processes: crystal growth of the optoelectronic material mercurous chloride, NASA Technical Memorandum 103788 (1991).
- [18] C. Mennetrier, W.M.B. Duval and N.B. Singh, Physical vapor transport of mercurous chloride under a nonlinear thermal profile, NASA Technical Memorandum 105920 (1992).
- [19] G.T. Kim, "Convective-diffusive transport in mercurous chloride (Hg_2Cl_2) crystal growth", *J. Ceramic Processing Research* 6 (2005) 110.
- [20] I. Catton, "Effect of wall conducting on the stability of a fluid in a rectangular region heated from below", *J. Heat Transfer* 94 (1972) 446.